

Electrically switchable whispering gallery mode lasing from ferroelectric liquid crystal microdroplets

Cite as: Appl. Phys. Lett. **114**, 091106 (2019); doi: [10.1063/1.5088863](https://doi.org/10.1063/1.5088863)

Submitted: 15 January 2019 · Accepted: 17 February 2019 ·

Published Online: 5 March 2019



View Online



Export Citation



CrossMark

Junaid Ahmad Sofi  and Surajit Dhara ^{a)} 

AFFILIATIONS

School of Physics, University of Hyderabad, Hyderabad 500046, India

^{a)}Electronic mail: sdsp@uohyd.ernet.in

ABSTRACT

Liquid crystal microdroplets have received considerable attention over recent years owing to their potential applications in chemical, biomedical sensing and lasing. We report experimental studies on whispering gallery mode lasing from dye-doped ferroelectric liquid crystal microdroplets suspended in a low refractive index and highly transparent perfluoropolymer at ambient temperature. We show that the lasing threshold pump energy of ferroelectric microdroplets is much lower than that of the nematic and cholesteric microdroplets. With the increasing electric field, the linewidth increases, while the lasing intensity decreases and eventually switches off beyond a particular field. Since the switching response time is fast ($\approx 350 \mu\text{s}$), ferroelectric liquid crystal based microlasers are useful for applications as electrically switchable sources in miniaturised devices and in soft photonic circuits.

Published under license by AIP Publishing. <https://doi.org/10.1063/1.5088863>

Transparent microspheres or microdroplets could behave as optical microcavities if their refractive indices are greater than those of dispersing media. In such systems, the light circulates inside the cavity due to the total internal reflection and the optical resonance occurs when the circulating light meets in-phase. In larger spheres, under a simple approximation, this can be achieved when $2\pi n_s \approx l\lambda$, where a is the radius, n_s is the refractive index of the sphere, and l is an integer.¹ This type of resonance is known as the whispering gallery mode (WGM) or morphology dependent resonance. They have small mode volumes and high quality factors (Q). The light source is usually a fluorescent dye, dispersed in the cavity and pumped by an external light source.^{1,2} If the pumping energy exceeds a certain threshold, the dye gives stimulated emission and the resonator emits multimode laser light. Liquid crystal microdroplets have drawn considerable attention across various scientific disciplines owing to their potential applications in tunable optical microcavities^{2–15} and sensors.^{16–22} They could well fit into the integrable photonics as essential optical components in miniaturised devices and hence serve widespread applications such as electrically or magnetically tunable lasers, filters, and sensors.

Humar *et al.* first demonstrated electrically tunable WGM resonance of nematic liquid crystal microdroplets.² Subsequently, they reported 3D lasing and chemical sensing as well.^{3,4} Later, Kumar *et al.* showed sensitive detection of nematic to smectic-A phase transition in

the microcavity.⁵ With the aim of exploring and expanding the versatile usage of liquid crystal droplets, we studied the electrical and thermal tuning of the quality factor (Q) and the free spectral range (FSR) of WGM resonance.⁶ We also reported on the magnetic field tuning of lasing in ferromagnetic nematic droplets.⁷ Among the liquid crystals, the ferroelectric liquid crystals (FLCs) show outstanding performance for fast electro-optical applications due to the spontaneous polarisation of the smectic layers. FLCs are especially attractive for low voltage operability, better optical contrast, bistability, and faster electro-optical response.^{23–32} At the backdrop of efforts on producing tunable and miniaturised lasers for diverse applications, we report experimental studies on electrically switchable lasing from room temperature ferroelectric liquid crystal microdroplets. It is expected that the switchable lasing adds diversity to the domain of optical components and could eventually make an important contribution in the race of fabrication of soft photonic chips.

We used a room temperature ferroelectric liquid crystal (KCFLC7S) procured from Kingston Chemicals Limited. It exhibits the following phase transitions: Cry. 5°C SmC* 73°C SmA* 100.5°C 114.5°C Iso. Its helical pitch at room temperature is about $2.8 \mu\text{m}$. The details of the mixture can be found in Refs. 25 and 26. We used a transparent perfluoropolymer CTX-809A commonly known as CYTOP diluted by a fluorinated solvent CT-Sol.180 at a 2:1 volumetric

mixing ratio for dispersing microdroplets of FLC.⁸ The polymer and the solvent were obtained from Asahi Glass Co. Ltd, Japan. CYTOP has a very low refractive index ($n = 1.34$) and provides shock free homeotropic alignment of smectic liquid crystals in cells.^{33–39} Recently, we have shown that CYTOP is a superior dispersing medium for forming spherical microdroplets with homeotropic alignment of the nematic director.⁸ Using a micropipette, FLC microdroplets with varying sizes were dispersed in CYTOP solution which was injected in cells made of two indium-tin-oxide coated glass plates separated by a spacer of thickness $240\ \mu\text{m}$. Before the dispersion, about 0.7 wt. % fluorescent dye (Nile red) was mixed with the FLC. An isolated microdroplet of desired size was chosen in the cell mounted on the sample stage of an inverted microscope (Nikon, Eclipse Ti-U) and was excited with the help of a Q-switched laser of wavelength $532\ \text{nm}$ (Teem Photonics, Model: PNG-M02010-130) with a pulse length of $400\ \text{ps}$, through a $60\times$ objective with $\text{NA} = 1.1$. The absorption band of Nile Red coincides with the pulsed laser. The light emitted from the selected microdroplet is collected by the same objective and sent to the high resolution spectrometer (Andor 500i). A schematic diagram of the cell is shown in Fig. 1(a). The details of the experimental setup are presented in our previous reports.^{5,6} For electric field studies, the dc

field is provided by a high voltage supply. The switching response time of lasing was measured with the help of a photomultiplier tube connected to a digital storage oscilloscope. A λ -plate retarder ($530\ \text{nm}$) was used to study the optical textures of the microdroplets. All the experiments were performed at room temperature.

Our study begins with the observation of microdroplets under a polarising optical microscope (POM) in the absence of any electric field. Images on the top row of Fig. 1 show POM micrographs of a few FLC microdroplets dispersed in CYTOP solution. The images underneath are taken with an additional λ -plate inserted at 45° with respect to the crossed polarisers. In smaller microdroplets (diameter $\lesssim 5.4\ \mu\text{m}$), four clear brushes are observed, suggesting that smectic layers are concentric and the layer normal is perpendicular to the interface. Thus CYTOP solution provides homeotropic surface anchoring to smaller FLC droplets. For larger droplets (diameter $\gtrsim 5.4\ \mu\text{m}$), the radial structure is not stable and a numeral 8 like defect line is formed near the central region [see λ -plate images in Figs. 1(d) and 1(e)]. With the increasing size, the defect appears like a hair pin and evolves from the centre towards the boundary [Figs. 1(f) and 1(g)]. The defect looks somewhat similar to that reported in cholesteric microdroplets, where two cores of $+1$ disclination lines forming a double helix structure fuse together in the center of the microdroplets and appear as a hair pin.^{40–45} The λ -plate images suggest that the textures of the larger FLC microdroplets are very complex. The equilibrium microdroplet structure results from the competition between the elastic forces which determines the layer orientation of the FLC in the bulk and the surface anchoring, which becomes dominant when the FLC is confined. For smaller microdroplets, the surface energy dominates and the radial structure is stable [Figs. 1(b) and 1(c)]. A schematic diagram of the cross-section of a microdroplet with concentric smectic layers is shown in Fig. 1(h). The molecules rotate in the layers along the helical axis that is orientated radially. The defect in the bigger FLC microdroplets is due to the geometric frustration of chiral ordering and similar to that is observed in cholesteric microdroplets, which essentially depends on the ratio of the pitch and the diameters of the microdroplets.

In what follows, we study the WGM resonance and lasing of the microdroplets under the excitation of the pulsed laser. Although smaller microdroplets appear radial and uniform, no WGM resonance is observed when the microdroplet diameter is lower than about $8\ \mu\text{m}$. This is presumably due to the dominant curvature losses that result from the unfulfilled requirement of the critical angle for light to travel through total internal reflection. Bigger microdroplets exhibit many modes and are often indistinguishable. Hence, in order to avoid the crowding of many modes, we confined our studies on isolated microdroplets with diameters in the range of $20\text{--}30\ \mu\text{m}$. Figure 2(a) shows the fluorescence image of an isolated droplet of diameter $22.7\ \mu\text{m}$ when pumped by the pulsed laser of energy $5\ \text{nJ}$. A faint light ring is observed surrounding the microdroplet, suggesting the excitation of WGMs. The corresponding spectra are presented in Fig. 2(c). It is observed that the WGM spectrum of FLC is significantly different from that usually observed in the case of nematic or smectic-A microdroplets.^{2,6,8} The modes have a lower linewidth and are not equally spaced. This is attributed to the inhomogeneity in the refractive index of the cavity that occurs due to the complex elastic deformation of the smectic layers. When the pump energy is increased sufficiently, we observe a clear bright ring with speckle formation [Fig. 2(b)]. The

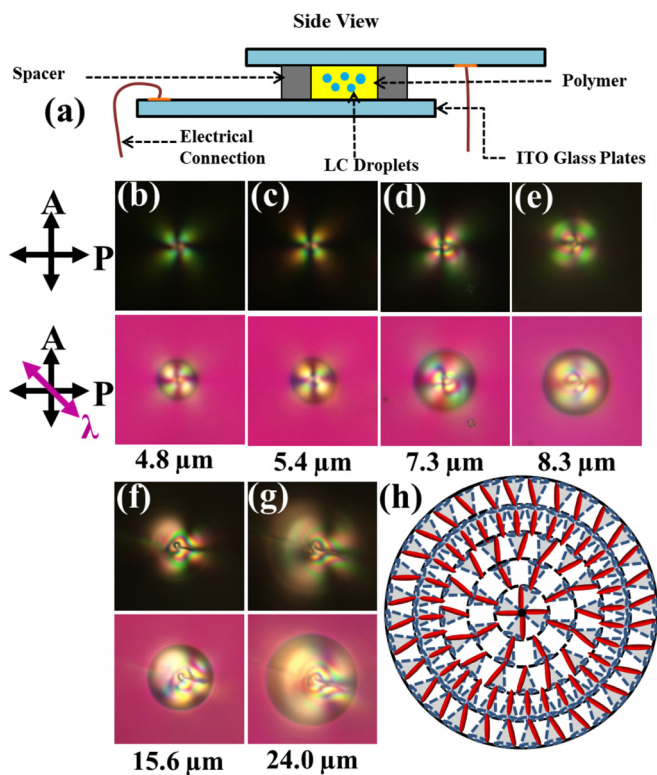


FIG. 1. (a) Schematic diagram of the cell made of two indium-tin-oxide (ITO) coated glass plates. Textures of FLC microdroplets of different diameters. (b)–(g) Images in the top row show polarising optical micrographs of droplets, while the bottom row shows the images taken using an additional λ -plate. The orientation of the slow axis of the λ -plate with respect to the crossed polarisers is shown on the left side. (h) Schematic diagram of the cross-section of a smaller droplet, showing concentric smectic layers with the radial helical axis. The red ellipsoids represent the molecules within the cone rotating along the helical axis.

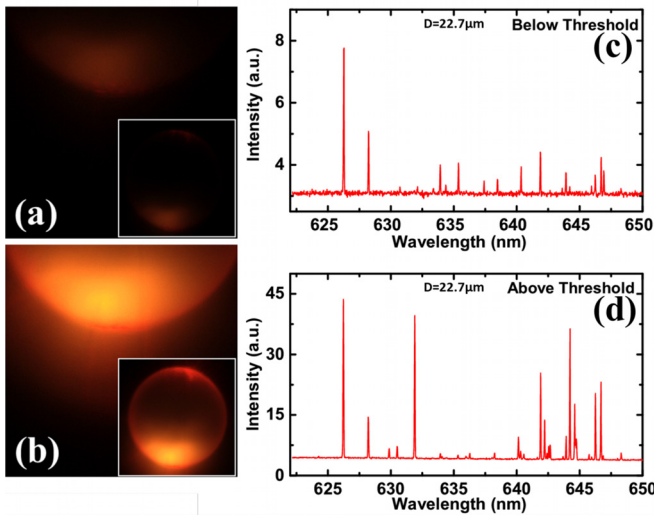


FIG. 2. WGM lasing of a Nile red dye doped FLC microdroplet of diameter $D = 22.7 \mu\text{m}$. Fluorescence images of the emission pattern at the droplet edge (a) at input energies of 5 nJ (below lasing threshold energy, discussed later) and (b) 60 nJ (above lasing threshold energy). (c) Typical WGM spectrum below threshold energy. (d) Corresponding spectrum above the lasing threshold energy. The insets show the images of the whole droplets.

corresponding spectrum is also shown in Fig. 2(d). It is noted that the peak intensities of the modes are increased significantly and some new modes are also visible. For example, the intensity of the dominant mode appearing at $\lambda = 626.27 \text{ nm}$ is increased from 7.8 to 44 (a.u.) when the pump energy is increased to 60 nJ. The speckle formation at the edge of the microdroplets is an indication of coherent emission in the microcavity.⁷

To characterise the spectrum, we measured the output intensity as well as the line-width of the modes as a function of input energy of a droplet of diameter $D = 23.8 \mu\text{m}$. Figure 3(a) shows that there is a clear threshold at 22 nJ, beyond which the output intensity of the mode ($\lambda = 626.3 \text{ nm}$) increases linearly. Figure 3(b) shows that the linewidth of the same mode decreases and becomes constant at the same threshold input energy. The threshold pump energy and line-width narrowing are important characteristics of laser emission. It is noticed that the threshold energy of the FLC is much smaller than that of the nematic and cholesteric liquid crystal microdroplets of comparable size and dye concentration. For example, the threshold pump energies for ferromagnetic nematic and cholesteric droplets are about 7 to 8 times higher than that of the FLC used in this experiment.^{4,7} The linewidth of the lasing in FLC microdroplets is close to 0.06 nm, and this is smaller compared to that reported (about 0.1 nm) in the two referred systems. These are attributed to the absence of strong director fluctuations in the FLC and also the low absorption of light by the FLC compared to nematic and cholesteric liquid crystals. Threshold pump energy also depends on the refractive index of the liquid crystals and the quantum yield of the dye, which depends on the medium, and hence, it may be more appropriate to compare the threshold values in liquid crystals having the same refractive index.

As a next step, we studied the effect of the dc electric field on the morphology and lasing of the FLC microdroplets. Figure 4 shows a

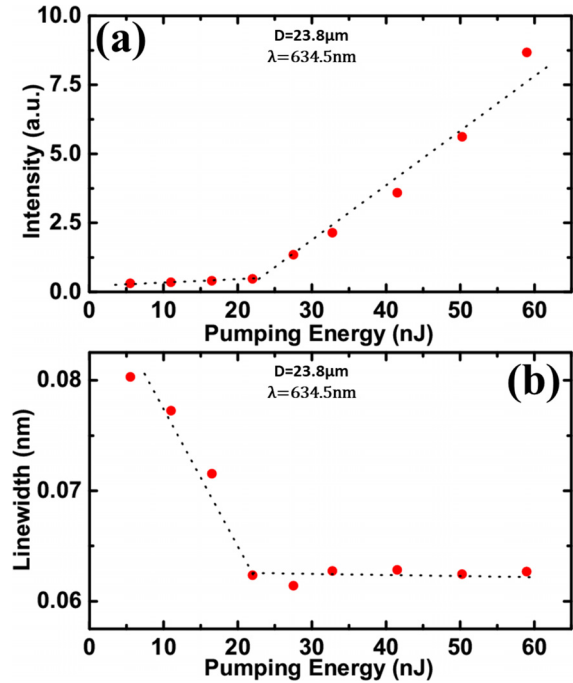


FIG. 3. (a) Intensity of a WGM peak ($\lambda = 634.5 \text{ nm}$) as a function of the input energy. A typical 2-slope lasing curve is observed. The dotted lines are added as guides to the eye, showing the lasing threshold at 22 nJ (b) Linewidth of the corresponding spectral peak as a function of input-pulse energy, showing reduction of the linewidth below the threshold energy. Droplet diameter $D = 23.8 \mu\text{m}$.

sequence of POM micrographs and the corresponding λ -plate images with the increasing electric field. The field is applied between two confining electrodes along the viewing direction. The textures of the microdroplets due to the applied field are very complex and harder to figure out. However, it is evident that the spontaneous electric polarisation of the layer is coupled to the external electric field, and consequently, the helix should unwind. The unwinding of the helix in the confined droplets is expected to deform the smectic layer orientation, which can increase the inhomogeneity of the refractive index. Figure 5(a) shows the effect of the electric field on the lasing spectrum from a microdroplet of diameter, $D = 20.1 \mu\text{m}$. The experiments were conducted at a fixed pumping energy of 60 nJ, which is much above the

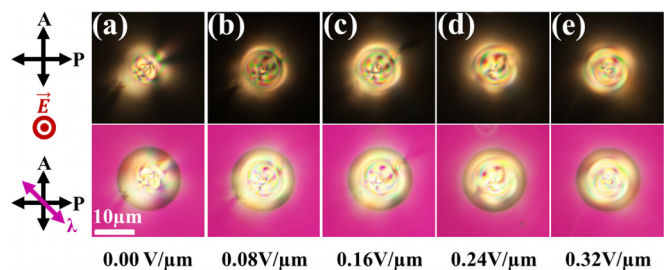


FIG. 4. Textures of an FLC microdroplet of diameter $D = 15.3 \mu\text{m}$ at various applied dc electric field strengths. The corresponding λ -plate images are shown underneath. The field direction is out of the plane.

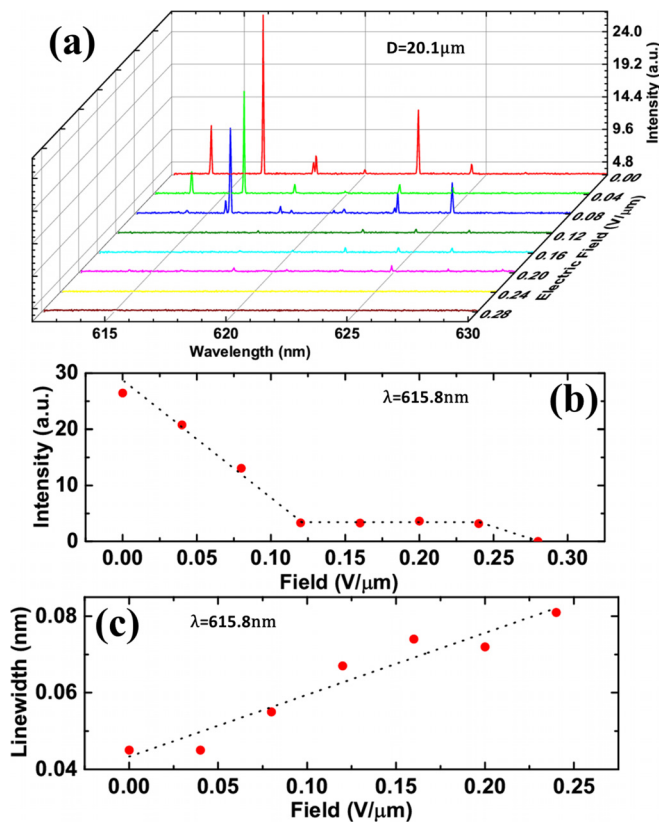


FIG. 5. (a) Effect of the dc electric field on the spectrum from an FLC droplet of diameter $D = 20.1 \mu\text{m}$. The intensity of the modes decreases with the increasing field. (b) Variation of emitted intensity corresponding to the dominant mode at $\lambda = 615.8 \text{ nm}$ and (c) linewidth as a function of field. The dotted line is drawn as a guide to the eye.

lasing threshold. Only a few lasing modes are observed, and the corresponding intensities decrease with the increasing field. The mode corresponding to the wavelength of $\lambda = 615.8 \text{ nm}$ is dominant compared to others. The intensity of this mode is shown as a function of field in Fig. 5(b). It decreases almost linearly up to a field of $0.12 \text{ V}/\mu\text{m}$, reaches a constant value by changing the slope, and eventually becomes zero beyond $0.28 \text{ V}/\mu\text{m}$. The lasing resumes again when the applied field is reduced to zero. The slope change at $0.12 \text{ V}/\mu\text{m}$ indicates that the lasing is switched off at this field, but the WGM modes are still present and eventually disappears beyond $0.28 \text{ V}/\mu\text{m}$. The measured switching response time at room temperature is $350 \pm 25 \mu\text{s}$.

For most of the microdroplets with diameters in the range of $15\text{--}30 \mu\text{m}$, the lasing is completely switched off within $0.3 \text{ V}/\mu\text{m}$. This is in contrast to the effect of the electric field on WGMs observed in the nematic microdroplets, wherein the modes survive at all fields but shift towards lower wavelength with the increasing field.^{2,8} The switching off lasing from the FLC microdroplets could be attributed to the significant optical energy loss due to the increased inhomogeneity of the refractive index, which occurs due to the enhanced deformation of the smectic layers as observed in Fig. 4. To get a qualitative notion of

the stated phenomenon, we looked at the corresponding effect on the line-width of the lasing of the same mode. It is noticed that the line-width increases almost linearly with the applied field [Fig. 5(c)]. This confirms that the energy loss in the microcavity increases with the applied field strength.

In conclusion, we studied WGM lasing from ferroelectric liquid crystal microdroplets at ambient temperature. The equilibrium structure of the microdroplets is size dependent. In smaller microdroplets, the smectic layers are concentric and almost free from elastic distortions but do not show any WGM resonance. The bigger microdroplets possess defect loops, and the overall structure is complex. As a result, the refractive index becomes inhomogeneous. The input threshold pump energy for the WGM lasing of FLC microdroplets is 7 to 8 times lower than that of the nematic and cholesteric microdroplets. The external electric field enhances the inhomogeneity of the refractive index further, and consequently, the optical energy loss in the cavity increases and eventually switches off the lasing. Because of fast switching speed, FLC could be used as an electrically switchable microlaser source in photonic soft-chips. FLC microdroplets could also be used as three-dimensional switchable Bragg type microresonators for omnidirectional lasing, but it is challenging to obtain perfectly radial orientation of the helical axis. The work in this direction is on progress and will be reported elsewhere.

We gratefully acknowledge the support from SERB (EMR/2015/001566) and DST (DST/SJF/PSA-02/2014-2015) and DST-PURSE(II). J.A.S. acknowledges UGC for the BSR fellowship.

REFERENCES

- ¹V. Kerry, *Optical Microcavities* (World Scientific, 2004).
- ²M. Humar, M. Ravnik, S. Pajk, and I. Musevic, *Nat. Photonics* **3**, 595 (2009).
- ³M. Humar and I. Musevic, *Opt. Express* **19**, 19836 (2011).
- ⁴M. Humar and I. Musevic, *Opt. Express* **18**, 26995 (2010).
- ⁵T. A. Kumar, M. A. Mohiddon, N. Dutta, N. K. Viswanathan, and S. Dhara, *Appl. Phys. Lett.* **106**, 051101 (2015).
- ⁶J. A. Sofi, M. A. Mohiddon, N. Dutta, and S. Dhara, *Phys. Rev. E* **96**, 022702 (2017).
- ⁷M. Marusa, J. A. Sofi, I. Kvasic, A. Mertelj, D. Lisjak, V. Niranjan, I. Musevic, and S. Dhara, *Opt. Express* **25**, 1073 (2017).
- ⁸J. A. Sofi and S. Dhara, "Stability of liquid crystal micro-droplets based optical microresonators," *Liq. Cryst.* (published online).
- ⁹A. Giorgini, S. Avino, P. Malara, P. De Natale, and G. Gagliardi, *Sci. Rep.* **7**, 41997 (2017).
- ¹⁰V. S. R. Jampani, M. Humar, and I. Musevic, *Opt. Express* **21**, 20506 (2013).
- ¹¹M. Humar, *Liq. Cryst.* **43**, 1937 (2016).
- ¹²I. Musevic, M. Skarbot, and M. Humar, *J. Phys. Condens. Matter* **23**, 284112 (2011).
- ¹³C. R. Lee, J. D. Lin, B. Y. Huang, T. S. Mo, and S. Y. Huang, *Opt. Express* **18**, 25896 (2010).
- ¹⁴J. D. Lin, M. H. Hsiegh, G. J. Wei, T. S. Mo, S. Y. Huang, and C. R. Lee, *Opt. Express* **21**, 15765 (2013).
- ¹⁵P. V. Shibaev, B. Crooker, M. Manevich, and E. Hanelt, *Appl. Phys. Lett.* **99**, 233302 (2011).
- ¹⁶S. Shivakumar, K. L. Wark, J. K. Gupta, N. L. Abbott, and F. Caruso, *Adv. Funct. Mater.* **19**, 2260 (2009).
- ¹⁷S. J. Woltman, G. D. Jay, and G. P. Crawford, *Nat. Mater.* **6**, 929 (2007).
- ¹⁸I. H. Lin, D. S. Miller, P. J. Bertics, C. J. Murphy, J. J. de Pablo, and N. L. Abbott, *Science* **332**, 1297 (2011).
- ¹⁹D. S. Miller and N. L. Abbott, *Soft Matter* **9**, 374 (2013).
- ²⁰M. Khan, A. R. Khan, J. H. Shin, and S. Y. Park, *Sci. Rep.* **6**, 22676 (2016).
- ²¹S. L. Lai, D. Hartono, and K. L. Yang, *Appl. Phys. Lett.* **95**, 153702 (2009).
- ²²A. D. Price and D. K. Schwartz, *J. Am. Chem. Soc.* **130**, 8188 (2008).

- ²³M. Hird, *Liq. Cryst.* **38**, 1467 (2011).
- ²⁴S. T. Lagerwall, *Ferroelectric and Antiferroelectric Liquid Crystals* (Wiley-VCH Verlag GmbH, Weinheim, Germany, 1999).
- ²⁵T. Joshi, A. Kumar, J. Prakash, and A. M. Biradar, *Liq. Cryst.* **37**, 1433 (2010).
- ²⁶A. Kumar, G. Singh, T. Joshi, G. K. Rao, A. K. Singh, and A. M. Biradar, *Appl. Phys. Lett.* **100**, 054102 (2012).
- ²⁷G. Hegde, P. Xu, P. Eugene, C. Vladimir, and H. S. Kwok, *Liq. Cryst.* **35**(9), 1137 (2008).
- ²⁸S. J. Elston, *J. Mod. Opt.* **42**, 19 (1995).
- ²⁹J. Y. Liu and K. M. Johnson, *IEEE Photonics Technol. Lett.* **7**, 1309 (1995).
- ³⁰A. L. Andreev, Y. P. Bobylev, N. A. Gubasaryan, I. N. Kompanets, E. P. Pozhidaev, T. B. Fedosenkova, V. M. Shoshin, and Y. P. Shumkina, *J. Opt. Technol.* **72**, 701 (2005).
- ³¹S. T. Lagerwall, *Ferroelectrics* **301**, 15 (2004).
- ³²C. Bahr, *Ferroelectric Properties and Electroclinic Effect* (Springer, New York, 2001).
- ³³S. Dhara, J. K. Kim, S. M. Jeong, R. Kogo, F. Araoka, K. Ishikawa, and H. Takezoe, *Phys. Rev. E* **79**, 060701 (2009).
- ³⁴S. M. Jeong, Y. Shimbo, F. Araoka, S. Dhara, N. Y. Ha, K. Ishikawa, and H. Takezoe, *Adv. Mater.* **22**, 34 (2010).
- ³⁵D. Venkata Sai, T. Arun Kumar, W. Haase, A. Roy, and S. Dhara, *J. Chem. Phys.* **141**, 044706 (2014).
- ³⁶T. Arun Kumar, P. Sathyanarayana, V. S. S. Sastry, H. Takezoe, N. V. Madhusudana, and S. Dhara, *Phys. Rev. E* **82**, 011701 (2010).
- ³⁷T. A. Kumar, K. V. Le, S. Aya, K. Fukuda, F. Araoka, K. Ishikawa, J. Watanabe, S. Dhara, and H. Takezoe, *Phase Trans.* **85**, 888 (2012).
- ³⁸T. Arun Kumar, V. S. S. Sastry, K. Ishikawa, H. Takezoe, N. V. Madhusudana, and S. Dhara, *Liq. Cryst.* **38**, 971 (2011).
- ³⁹J. K. Kim, S. M. Jeong, S. Dhara, F. Araoka, K. Ishikawa, and H. Takezoe, *Appl. Phys. Lett.* **95**, 063505 (2009).
- ⁴⁰T. Orlova, S. J. Abhoff, T. Yamaguchi, N. Katsonis, and E. Brasselet, *Nat. Commun.* **6**, 7603 (2015).
- ⁴¹G. Posnjak, S. Copar, and I. Musevic, *Nat. Commun.* **8**, 14594 (2017).
- ⁴²E. Bukusoglu, X. Wang, Y. Zhou, J. A. Martinez-Gonzalez, M. Rahimi, Q. Wang, J. J. de Pablo, and N. L. Abbott, *Soft Matter* **12**, 8781 (2016).
- ⁴³Y. Zhou, E. Bukusoglu, J. A. Martinez-Gonzalez, M. Rahimi, T. F. Roberts, R. Zhang, X. Wang, N. L. Abbott, and J. J. de Pablo, *ACS Nano* **10**, 6484 (2016).
- ⁴⁴D. Sec, T. Porenta, M. Ravnik, and S. Zumer, *Soft Matter* **8**, 11982 (2012).
- ⁴⁵O. O. Prishchepa, V. Y. Zyryanov, A. P. Gardymova, and V. F. Shabanov, *Mol. Cryst. Liq. Cryst.* **489**, 84 (2008).